Supporting Information

Enhancement of biexciton emission due to long-range interaction of single quantum dots and gold nanorods in a thin-film hybrid nanostructure

Victor Krivenkov[*,1], *Simon Goncharov*[1], *Pavel Samokhvalov*[1], *Ana Sánchez-Iglesias*[2], *Marek Grzelczak*[3], *Igor Nabiev*[1,4], *and Yury Rakovich*[*,1,3,5,6]

[1] National Research Nuclear University MEPhI (Moscow Engineering Physics Institute), 115409 Moscow, Russian Federation

[2] CIC biomaGUNE, Paseo de Miramón 182, 20014 Donostia-San Sebastián, Spain

[3] Donostia International Physics Center, Paseo Manuel Lardizabal 4, 20018 Donostia-San Sebastián, Spain

[4] Laboratoire de Recherche en Nanosciences, LRN-EA4682, Université de Reims Champagne-Ardenne, 51100 Reims, France

[5] Centro de Física de Materiales (MPC, CSIC-UPV/EHU) and Donostia International Physics Center, Paseo Manuel de Lardizabal 5, 20018 Donostia - San Sebastian, Spain

[6] IKERBASQUE, Basque Foundation for Science, Maria Diaz de Haro 3, 48013 Bilbao, Spain

1. Materials

In this study we used the QDs with a CdSe core and ZnS/CdS/ZnS QD-multishells in a hexane solution. The synthesis of QDs was carried out according to the procedure described elsewhere.[1] Figure S1a shows the PL and extinction spectra of the synthesized QDs. Their TEM image is shown in Figure S1b. The synthesized QDs had a core size of 2.3 nm, which was calculated before the shell formation using the previously developed method.[2] After growing the shell, the average size has been estimated from TEM images and was about 5 nm. The hydrodynamic diameter of the QDs in hexane was also 5 nm, as follows from the data obtained using a Malvern Zeta Sizer ZS. The relative QY of the QDs in hexane has been determined by comparison of QD fluorescence with a fluorescence of Rhodamine 6G in methanol and was estimated to be 90%.

Gold nanorods (GNRs) were prepared using Ag-assisted seeded growth.[3] Seeds were prepared by the fast reduction of $HAuCl_4$ (5 mL, 0.25 mM) with freshly prepared $NaBH_4$ (0.3 mL, 10 mM) in an aqueous CTAB solution (100 mM). The seed solution was aged at room temperature for 30 min before use. To prepare the growth solution, 7.0 g of CTAB and 1.234 g of NaOL were dissolved in 250 mL of warm water (~50 °C). The solution was cool down to 30 °C followed the addition of $AgNO_3$ (18 mL, 4 mM). The mixture was kept undisturbed at 30 °C for 15 min after which was added $HAuCl_4$ solution (250 mL, 1 mM). Once the solution became colorless, HCl (1.5 mL, 37 wt. % in water) and ascorbic acid (1.25 mL, 64 mM) were added and the mixture was stirred for 30 s. Finally, seed solution (0.4 mL) was injected into the growth solution under vigorous stirring. After 30 s the mixture was left undisturbed at 30°C for 12 h. The final gold nanorods were isolated by centrifugation at 7.000 rpm for 30 min and redispersed in CTAB 100mM.

The maximum of the localized surface plasmon resonance (LSPR) of the initial gold nanorods was 709 nm. The gold nanorods of low aspect ratio were obtained using our previously reported method.[4] Briefly, Au^{+3}-CTAB complex (6.85 mL, [Au] = 1 mM, [CTAB] = 100 mM,) was added dropwise under magnetic stirring to the Erlenmeyer flask containing 100 mL of the initial gold nanorods ([Au] = 0.25 mM, [CTAB] = 100 mM). The solution was allowed to react at 30 °C for 1 h. Then, the solutions were centrifuged twice (8000 rpm, 30 min) to remove excess gold salt and redispersed in CTAB solution (15 mM) to reach final gold concentration equal to 1 mM. The size of the short gold nanorods was 39.1 ± 1.3 by 20.5 ± 0.5 nm. The extinction spectrum of nanorods is presented in Figure S1a and TEM image of the nanorods is shown in Figure S1c.

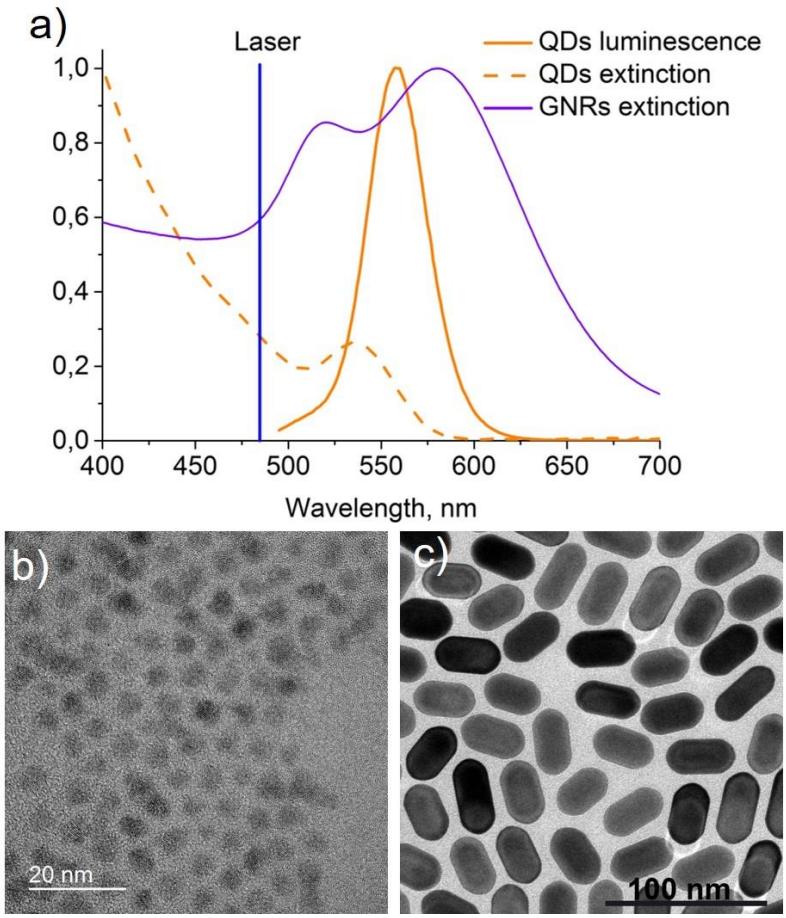

Figure S1. a) The extinction spectra of a hexane solution of QDs (the dashed line) and an aqueous solution of nanorods (the purple line). The PL spectrum of the QDs is shown by a solid orange line. b) and c) TEM image of CdSe/ZnS/CdS/ZnS quantum dots and gold nanorods, respectively.

2. Fabrication of PMMA-QD-PMMA thin films

To fabricate thin-film hybrid structures, we employed the method of layer-by-layer spin-coating using a Model KW-4A Spin Coater. Poly(methyl methacrylate) (PMMA) with an average molecular weight of ~120,000 by GPC (Sigma Aldrich, 182230) was used to prepare polymer films on a glass substrate. The thickness of the PMMA layers was estimated using the AFM height profiling method after cutting off part of the deposited film (Figure S2).

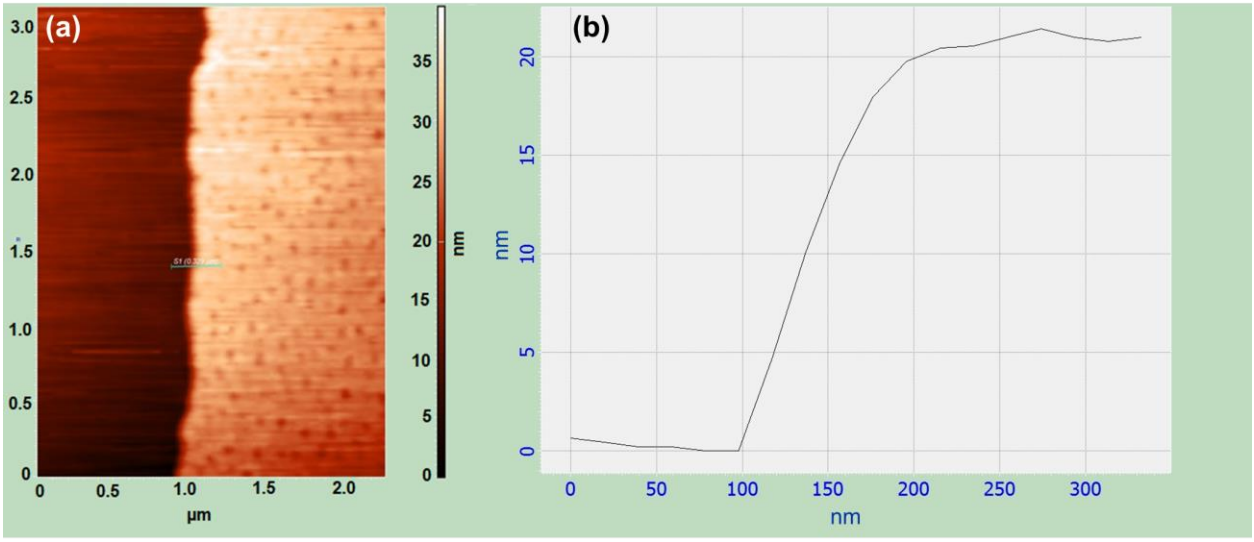

Figure S2. Imaging and measurement of PMMA film thickness using AFM height profiling after cutting off part of the deposited film. (a) AFM image of film in the cut-off area. (b) The measured difference in height of the structure in the cut-off area.

First, the thickness of the PMMA layer deposited directly on the cover glass from 70 µL of a 0.4 wt% PMMA solution at 3500 rpm was estimated, yielding a value of ~5 nm (Figure S2). Then QDs from 70 µL of a $3 \cdot 10^{-11}$ M hexane solution were deposited on

top of the first PMMA layer at 3500 rpm. After that, the second layer of PMMA was deposited at 1000 rpm using 70 μL of the 0.4 wt% solution (Figure S3, Scheme 1). The measured thickness of the two layers was ~20 nm. The same deposition procedure using the 0.2 wt% solution yields a thickness of ~10 nm (Figure S3, Scheme 2).

For more accurate control of the distance between the QDs and GNRs the procedure for deposition of PMMA layers was modified (Figure S3, Scheme 2). As in the previous case, a 5-nm PMMA layer was first spin-coated on a cover glass followed by the spin-coating of QDs. Then the next layer of 0.2 wt% PMMA solution was spin-coated, so that the total thickness of the structure was 10 nm. After that, the PMMA spacer layer was deposited on top of it, and the distance between the QDs and GNRs was estimated as the thickness of the resulting structure minus 10 nm. Using this strategy, a number of films with a total thickness from 10 (no spacer) to 180 nm were fabricated. The thickness calibration curve for the structures with spacer deposited at 1000 rpm and whole thickness up to 140 nm shown at Figure S4. The film structure with maximum total thickness of 180 nm was fabricated by deposition of the third layer with 3 wt% PMMA solution at 600 rpm.

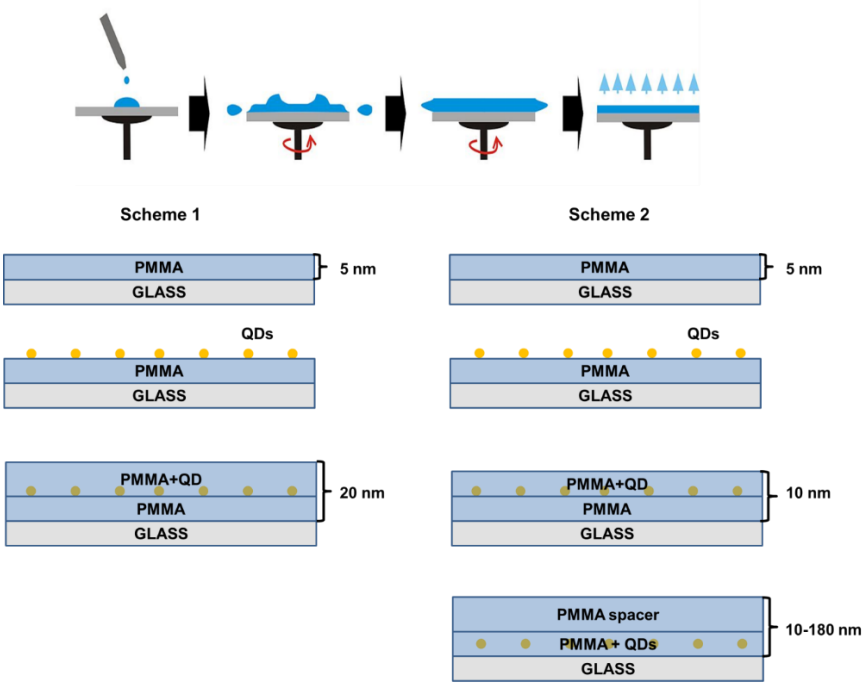

Figure S3. Fabrication schemes 1 and 2 for the PMMA-QD-PMMA thin-film hybrid structures.

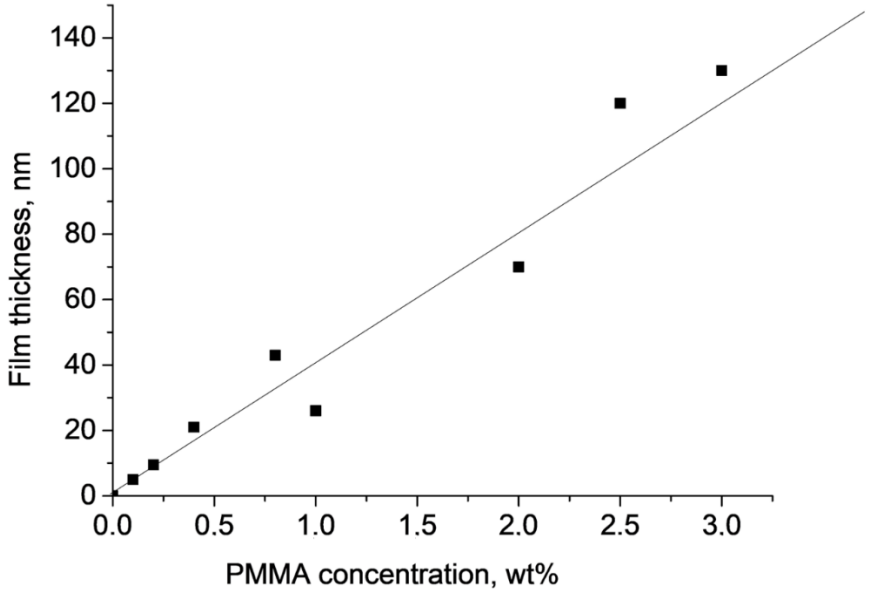

Figure S4. Dependence of the total thickness of the hybrid structure, made by spin-coating of the PMMA solution over the 10 nm PMMA film, on the PMMA solution weight concentration.

3. Setup and methods used for single QD studies

To study the emission properties of single QDs, a Micro Time 200 scanning confocal time-resolved fluorescent microscope setup (PicoQuant) was used, the optical scheme of which is shown in Figure S5.

A 485-nm diode laser working in a pulse regime with repetition rate of 5 MHz and a pulse duration of ~100 ps was used for the PL excitation. The average excitation power was up to 3 μW, which corresponds to a pulse energy below 0.6 pJ and ensures the non-saturated PL regime.[5] The laser beam was focused on the sample using a UPLSAPO 60XW Plan Apochromat water-immersion objective lens with NA = 1.2. The PL was collected by the same objective lens and then passed through a dichroic mirror and an optical filter, which cut off the laser line. Then, the PL signal was focused on a 150-μm pinhole and sent to a 50/50 beamsplitter. In each arm after the beamsplitter, the beam was focused on an avalanche photodiode. The signal from the photodiodes was recorded by a Hydra Harp 400 electronic module.

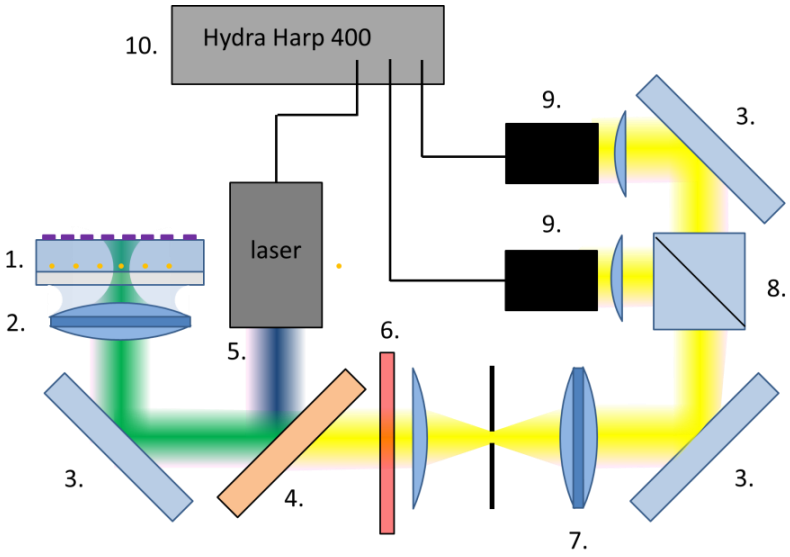

Figure S5. Optical scheme of the confocal time-resolved fluorescent microscope Micro Time 200 used for measurement of fluorescence properties of single QD. 1- thin film sample; 2 – water immersion objective with 1.2 NA; 3 – mirrors; 4 – dichroic mirror; 5

– 485 nm diode laser with 100 ps pulse duration; 6 - optical filter cutting off the laser line; 7 - 150 µm pinhole; 8 – beam splitter; 9 – two avalanche photodiodes; 10 – Hydra Harp 400 multichannel time-correlated single photon counting module.

The use of scanning confocal fluorescent imaging, made it possible to estimate the number of single QDs and their aggregates. It was found that the surface density of QDs in the structure does not exceed 0.5 μm^{-2}, while a rather large number of single QDs are observed (Figure S6). This surface density ensures that the average distance between individual QDs is larger than the laser excitation spot (~350 nm).

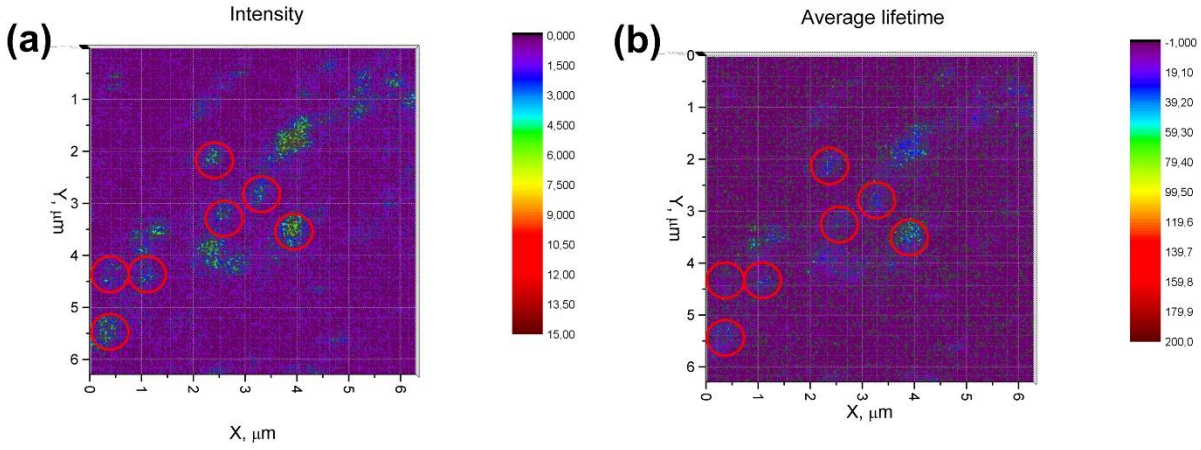

Figure S6. Fluorescence images of QDs in the PMMA film: (a) fluorescent intensity image, (b) fluorescent lifetime image.

4. Investigation of the emission properties of the same single QD before and after GNR deposition.

To study the emission properties of the same single QD before and after GNRs deposition, the following procedure was implemented (Figure S7a). First, the objective lens was focused on a single QD, and its time-resolved PL intensity, PL decay kinetics and second-order cross correlation function were measured (see Section 5). Then, 20 µL of an aqueous solution of GNRs with a concentration of 10^{-9} M was dropped on top of the structure and left to dry completely. The resulting GNRs layer was thick enough and

covered all the surface of the region of interest (Figure S8) to ensure that each QD in the PMMA film is in close proximity to the GNRs. Then, the emission properties of the same QD were studied again (Figure S7a). Since drying usually leads to the aggregation of a certain amount of GNRs, the extinction spectra of 10 fabricated GNR films were measured separately. The mean maximum of plasmon resonance was observed at 610 nm with a standard deviation of 20 nm. Figure S7b shows a representative spectrum of a GNRs film. It can be seen that the plasmonic band still considerably overlaps with the PL spectrum of the QDs.

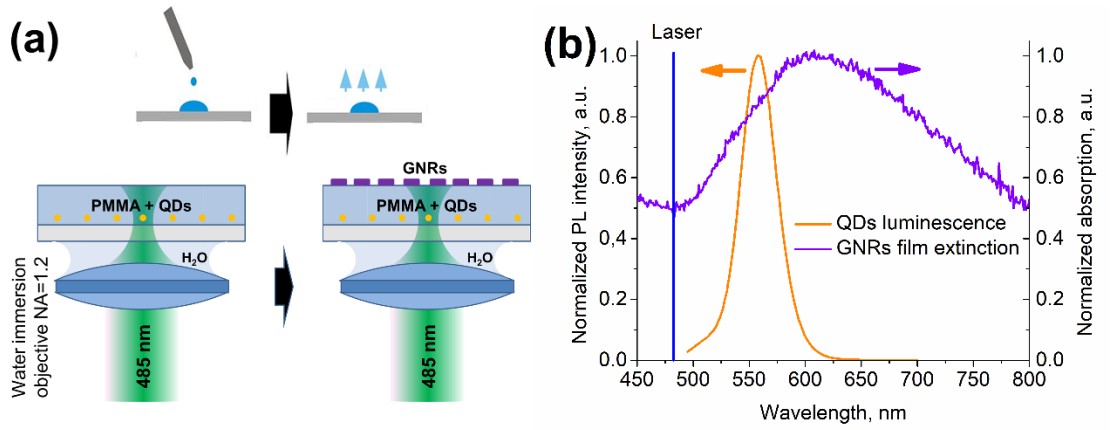

Figure S7. (a) Schematics of fabrication of the hybrid QD-GNR during PL experiments on a single QD; (b) A representative extinction spectrum of a dried GNR film (blue line) and the PL band of the QDs (orange line). The vertical lane indicates the spectral position of the excitation laser.

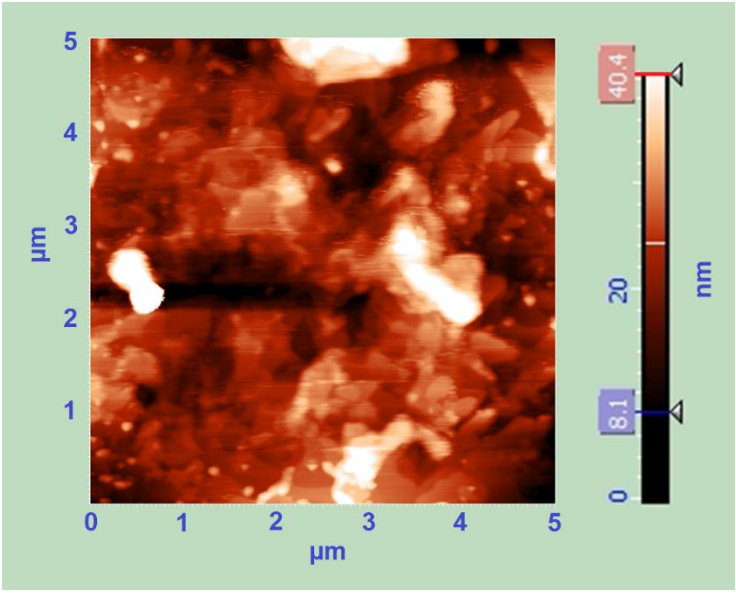

Figure S8. AFM image of distribution of gold nanorods on the surface of PMMA-QD-PMMA thin film hybrid structure.

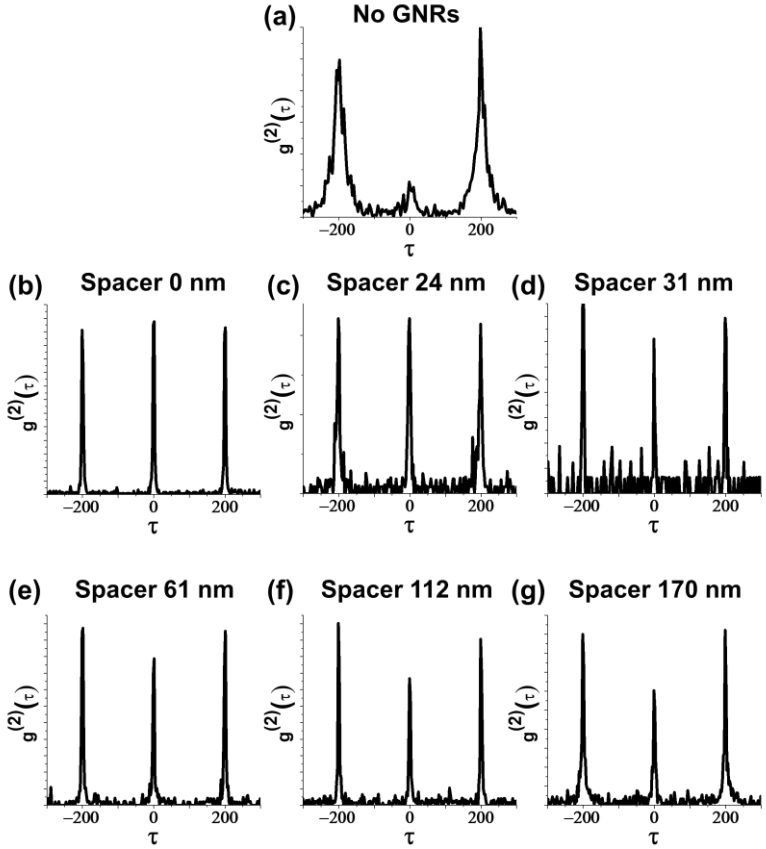

Figure S9. The characteristic cross-correlation functions of a single QD: (a) before GNRs deposition, and in presence of GNRs separated from QDs by PMMA spacer with thickness: (b) 0 nm, (c) 24 nm, (d) 31 nm, (e) 61 nm, (f) 112 nm, (g) 170 nm.

Table S1. Ratio of the area of the central peak to the average area of the side peaks of the cross-correlation function at different thickness of the PMMA spacer between the QD and GNRs.

No	Spacer thickness, nm	Ratio of the area of the central peak to the average area of the side peaks	Calculation error
1	No GNRs	0.1-0.3	0.05-0.15
2	0	0.959	0.097
3	24	0.968	0.14
4	24	0.916	0.171
5	31	0.892	0.186
6	61	0.865	0.115
7	61	0.823	0.117
8	112	0.834	0.136
9	112	0.822	0.101
10	170	0.712	0.063

5. Investigation of PL decay kinetics and PCS

The same setup but with only one detector was used to study the PL decays. All decay curves recorded in time-resolved PL experiments were approximated by the following equation

$$I(t) = \sum_i A_i \cdot e^{-t/\tau_i}, \text{ (S1)}$$

where I is the intensity, t is the time, and τ_i are the PL decay times.

To compare the temporal characteristics of PL in different samples, the parameter τ_{awl} was used, which is an amplitude-weighted average lifetime and can be expressed as

$$\tau_{awl} = \frac{\sum_i A_i \cdot \tau_i}{\sum_i A_i}. \text{ (S2)}$$

Unlike the traditionally used intensity-weighted average lifetime, the amplitude-weighted average lifetime is proportional to the average value of QY.[6]

To ensure the detection of PL from a single QD, the PCS based on the measurement of the photon coincidence correlation was used.

The main parameter is the second-order cross correlation function $g^{(2)}(\tau)$, measured by splitting PL signal into two detectors. This function is calculated by the following equation:

$$g^{(2)}(\tau) = \frac{<I_1(t)I_2(t+\tau)>}{<I_1(t)><I_2(t+\tau)>}, \text{ (S3)}$$

where $I_1(t)$ is the temporal signal from the first detector, $I_2(t)$ is the signal from the second detector, and τ is the time delay between them.

REFERENCES

1. Linkov, P.; Krivenkov, V.; Nabiev, I.; Samokhvalov, P. High Quantum Yield CdSe/ZnS/CdS/ZnS Multishell Quantum Dots for Biosensing and Optoelectronic Applications. *Materials Today: Proceedings* **2016,** *3* (2), 104-108.
2. Jasieniak, J.; Smith, L.; van Embden, J.; Mulvaney, P.; Califano, M. Re-examination of the Size-Dependent Absorption Properties of CdSe Quantum Dots. *J. Phys. Chem. C* **2009,** *113* (45), 19468–19474.
3. Ye, X.; Zheng, C.; Chen, J.; Gao, Y.; Murray, C. B. Using Binary Surfactant Mixtures To Simultaneously Improve the Dimensional Tunability and Monodispersity in the Seeded Growth of Gold Nanorods. *Nano Lett.* **2013,** *13* (2), 765-771.
4. Simon, T.; Melnikau, D.; Sánchez-Iglesias, A.; Grzelczak, M.; Liz-Marzán, L. M.; Rakovich, Y.; Feldmann, J.; Urban, A. S. Exploring the Optical Nonlinearities of Plasmon-Exciton Hybrid Resonances in Coupled Colloidal Nanostructures. *The Journal of Physical Chemistry C* **2016,** *120* (22), 12226-12233.
5. Matsuzaki, K.; Vassant, S.; Liu, H.-W.; Dutschke, A.; Hoffmann, B.; Chen, X.; Christiansen, S.; Buck, M. R.; Hollingsworth, J. A.; Götzinger, S.; Sandoghdar, V. Strong plasmonic enhancement of biexciton emission: controlled coupling of a single quantum dot to a gold nanocone antenna. *Sci. Rep.* **2017,** *7*, 42307.
6. Lakowicz, J. R. *Principles of Fluorescence Spectroscopy*. 3rd ed.; Kluwer Academic: New York, 2006; p 954.